Turk J Elec Eng & Comp Sci, Vol.20, No.Sup.1, 2012, © TÜBİTAK
doi:10.3906/elk-1102-1047

Optimal design of UPFC-based damping controller using imperialist competitive algorithm

Ali AJAMI[1,*], **Reza GHOLIZADEH**[2]
[1] *Electrical Engineering Department, Azarbaijan Shahid Madani University, Tabriz-IRAN*
e-mail: ajami@azaruniv.edu
[2] *Young Researchers Club, Islamic Azad University, Ardabil Branch, Ardabil-IRAN*

Received: 15.02.2011

Abstract

In this paper, the optimal design of supplementary controller parameters of a unified power flow controller (UPFC) to damp low-frequency oscillations in a weakly connected system is investigated. The individual design of the UPFC controller, using the imperialist competitive algorithm (ICA) technique over a wide range of operating conditions, is discussed. The effectiveness and validity of the proposed controller on damping low-frequency oscillations is tested through a time-domain simulation and eigenvalue analysis under 4 loading conditions and a large disturbance. The simulation results, carried out using MATLAB/Simulink software, reveal that the tuned ICA-based UPFC controller has an excellent capability of damping power system low-frequency oscillations and greatly enhances the dynamic stability of the power systems.

Key Words: *Power system stability, low-frequency oscillation damping, UPFC, multipoint optimization, imperialist competitive algorithm*

1. Introduction

Presently, power demand is growing dramatically and the extension in transmission and generation is restricted with the rigid environmental constraints and limited availability of resources. As a result, power systems of today are far more loaded than before. This brings about the necessity for power systems to be operated near their stability limits. Moreover, interconnection between remotely located power systems gives rise to low-frequency oscillations in the range of 0.1-0.3 Hz. If not well damped, these oscillations may keep growing in magnitude, resulting in a loss of synchronism [1].

Power system stabilizers (PSSs) have been used over the recent decades to serve the purpose of improving power system damping to low-frequency oscillations. PSSs have proven to be efficient in performing their assigned tasks, which operate on the excitation system of generators. However, PSSs may unfavorably have an effect on the voltage profile, may result in a leading power factor, and may be unable to control oscillations caused by large disturbances [1].

*Corresponding author: Electrical Engineering Department, Azarbaijan Shahid Madani University, Tabriz-IRAN

Flexible AC transmission system (FACTS) devices, when used to improve power system steady-state performance, have shown very encouraging results. FACTS devices can cause a substantial increase in power transfer limits during steady state through the modulation of bus voltage, phase shift between buses, and transmission line reactance. Owing to the extremely fast control action associated with FACTS device operations, they have been very promising candidates for utilization in the power system damping enhancement.

The unified power flow controller (UPFC) can be used for power flow control, loop flow control, load sharing among parallel corridors, enhancement of transient stability, mitigation of system oscillations, and voltage (reactive power) regulation [2,3]. Performance analysis and control synthesis of the UPFC require its steady-state and dynamic models. A 2-source UPFC steady-state model including source impedances is suggested in [4]. Under the assumption that the power system is symmetrical and operates under 3-phase balanced conditions, a steady-state model, a small-signal linearized dynamic model, and a state-space large-signal model of a UPFC were developed in [5]. Wang developed 2 UPFC models [6,7] in 1999, which have been linearized and incorporated into the Phillips-Heffron model. The UPFC damping controller design can be found in [1,8-12]. The supplementary controller can be applied to the shunt inverter through the modulation index of the reference voltage signal or to the series inverter through the modulation of the power reference signal. In [1] and [12], the particle swarm optimization (PSO) algorithm is used for tuning the optimum parameter settings of UPFC controllers for power system oscillation damping. The authors of [13] employed the real-coded genetic algorithm to optimize the damping controller parameters of the UPFC. In [14], bacterial foraging was used for the UPFC lead-lag type of controller parameter design.

Lee and Sun in [15] used the linear quadratic regulator method to design the state feedback gain of the static synchronous compensator (STATCOM) controller to increase the damping of a single-machine infinite-bus (SMIB) power system. An adaptive improved PSO hybrid with simulated annealing was applied to the design of a UPFC damping controller in [14]. Comparison of the PSS, static VAR compensator, and STATCOM controllers for damping power system oscillations using the Hopf bifurcation theory, an "extended" eigenvalue analysis to study different controllers, their locations, and the use of various control signals for the effective damping of these oscillations was presented in [10].

In this paper, the imperialist competitive algorithm (ICA) is used for the optimal tuning of a UPFC-based damping controller in order to enhance the damping of a power system's low-frequency oscillations and achieve the desired level of robust performance under different operating conditions, as well as different parameter uncertainties and a disturbance. The ICA is a new heuristic algorithm for global optimization searches that is based on imperialistic competition [17]. Over the last 5 years, after it was first introduced, this algorithm has been used in a variety of research areas [18-22] and has been proven as a promising tool for optimization purposes. According to [17] and [21], the ICA has better results than the genetic algorithm (GA) and PSO, respectively.

In this study, the ICA technique is used for the first time for UPFC damping controller design. The controller is automatically tuned with optimization of an eigenvalue-based objective function using the ICA to simultaneously shift the lightly damped and undamped electromechanical modes to the left side of the s-plane, such that the relative stability is guaranteed and the time-domain specifications are simultaneously secured.

2. Description of the ICA algorithm

The ICA is a new heuristic algorithm for global optimization searches that is based on imperialistic competition [17]. The ICA, similar to other heuristic algorithms such as PSO, GA, etc., starts with an initial population that is called a country. The initial population is divided into 2 types of colonies and imperialists, which together organize empires. The introduced evolutionary algorithm is constituted by imperialistic competition among these empires. During times of competition, the weak empires fall and the strong empires take possession of their colonies. Finally, this competition converges to a state in which the colonies have the same cost function value, called the imperialist, and there is only one empire. After all of the colonies are divided among the imperialists and the initial empires are created, these colonies move toward their related imperialist state as an assimilation policy [17]. The movement of a colony toward the imperialist is shown in Figure 1, where d is the distance between the colonies and the imperialist, and θ and x represent random numbers with uniform distribution, as given in Eq. (1).

$$x \approx U(0, \beta \times d), \qquad \theta \approx U(-\gamma, \gamma) \tag{1}$$

In the above equation, the terms β and γ describe parameters that modify the area that colonies randomly search around the imperialist. The total cost of all of the empires can be computed from Eq. (2). More descriptions about the ICA and the pseudocode of the ICA can be found in [17].

$$T.C.n = \ Cost\ (imperialist\ _n) + \zeta_{ica} mean\{Cost(colonies\ of\ empire\ _n)\} \tag{2}$$

The ICA, as a new heuristic algorithm, is used in multiple applications, such as PID controller designing [18], optimal placement of FACTS devices [19], economic load dispatch of power systems [20], power system stabilization [21], or harmonic elimination in multilevel inverters [22].

In this paper, the ICA is used to obtain the optimal values of the supplementary controller parameters of a UPFC.

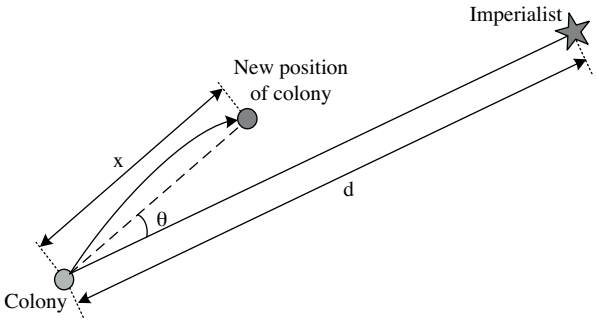

Figure 1. Movement of colonies toward their related imperialist [17].

3. Mathematical model of power system with UPFC

Figure 2 shows the test power system with a UPFC. In this paper, the test power system is a SMIB with 2 parallel lines. It can be seen from Figure 2 that the UPFC has 4 input control signals. These control signals are m_E, m_B, δ_E, and δ_B. The parameters of the test power system are given in the Appendix.

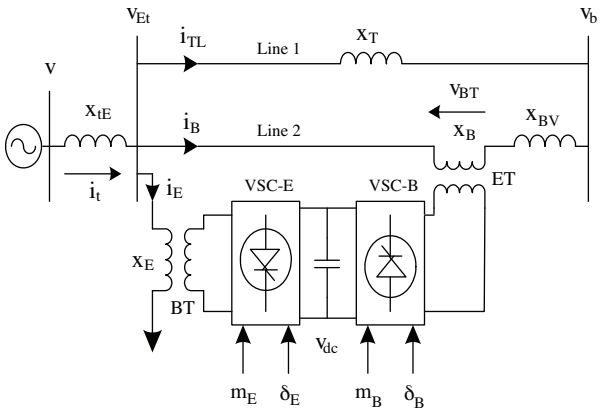

Figure 2. Test power system with UPFC.

3.1. Nonlinear model of test power system

In this section, to study the effect of the UPFC in the small-signal stability improvement of a power system, a dynamic model of a UPFC is presented. While neglecting the resistance and transients of the excitation (ET) and boosting (BT) transformers in Figure 2, the UPFC model in the dq reference frame can be obtained as [1,4,6,12]:

$$\begin{bmatrix} v_{Etd} \\ v_{Etq} \end{bmatrix} = \begin{bmatrix} 0 & -x_E \\ x_E & 0 \end{bmatrix} \begin{bmatrix} i_{Ed} \\ i_{Eq} \end{bmatrix} + \begin{bmatrix} \frac{m_E \cos\delta_E v_{dc}}{2} \\ \frac{m_E \sin\delta_E v_{dc}}{2} \end{bmatrix} \tag{3}$$

$$\begin{bmatrix} v_{Btd} \\ v_{Btq} \end{bmatrix} = \begin{bmatrix} 0 & -x_B \\ x_B & 0 \end{bmatrix} \begin{bmatrix} i_{Bd} \\ i_{Bq} \end{bmatrix} + \begin{bmatrix} \frac{m_B \cos\delta_B v_{dc}}{2} \\ \frac{m_B \sin\delta_B v_{dc}}{2} \end{bmatrix} \tag{4}$$

$$\begin{aligned} \dot{v}_{dc} = {} & \tfrac{3m_E}{4C_{dc}} \begin{bmatrix} \cos\delta_E & \sin\delta_E \end{bmatrix} \begin{bmatrix} i_{Ed} \\ i_{Eq} \end{bmatrix} + \\ & \tfrac{3m_B}{4C_{dc}} \begin{bmatrix} \cos\delta_B & \sin\delta_B \end{bmatrix} \begin{bmatrix} i_{Bd} \\ i_{Bq} \end{bmatrix}. \end{aligned} \tag{5}$$

In the above equations, v_{Et}, i_E, v_{Bt}, and i_B represent the voltage and current of the excitation and boosting transformers, respectively, and v_{dc} andC_{dc} show the DC link voltage and DC link capacitance, respectively.

When considering the circuit equations of Figure 2 and some simplifications, the currents of the excitation and boosting transformers and line 2 in the dq reference frame can be written as:

$$i_{TLd} = \frac{1}{x_T}\left(x_E i_{Ed} + \frac{m_E \sin\delta_E v_{dc}}{2} - v_b \cos\delta\right), \tag{6}$$

$$i_{TLq} = \frac{1}{x_T}\left(x_E i_{Eq} - \frac{m_E \cos\delta_E v_{dc}}{2} + v_b \sin\delta\right), \tag{7}$$

$$i_{Ed} = \frac{x_{BB}}{x_{d2}} E'_q + x_{d7}\frac{m_B \sin\delta_B v_{dc}}{2} + x_{d5} v_b \cos\delta + x_{d6}\frac{m_E \sin\delta_E v_{dc}}{2}, \tag{8}$$

$$i_{Eq} = x_{q7}\frac{m_B \cos\delta_B v_{dc}}{2} + x_{q5} v_b \sin\delta + x_{q6}\frac{m_E \cos\delta_E v_{dc}}{2}, \tag{9}$$

$$i_{Bd} = \frac{x_E}{x_{d2}} E'_q - \frac{x_{d1}}{x_{d2}}\frac{m_B \sin\delta_B v_{dc}}{2} + x_{d3} v_b \cos\delta + x_{d4}\frac{m_E \sin\delta_E v_{dc}}{2}, \tag{10}$$

$$i_{Bq} = \frac{X_{q1}}{X_{q2}}\frac{m_B \cos\delta_B V_{dc}}{2} + X_{q3} V_b \sin\delta + X_{q4}\frac{m_B \cos\delta_B V_{dc}}{2}, \tag{11}$$

where x_E and x_B represent the leakage reactance of the ET and BT, respectively, and the reactances x_{qE}, x_{dE}, x_{BB}, $x_{d1} - x_{d7}$, and $x_{q1} - x_{q7}$ are given in [23].

The conventional nonlinear dynamic equations of the generator shown in the SMIB test system in Figure 2 are:

$$\dot{\delta} = \omega_b (\omega - 1), \tag{12}$$

$$\dot{\omega} = (P_m - P_e - D(\omega - 1))/M, \tag{13}$$

$$\dot{E}'_q = \left(E_{fd} - (x_d - x'_d) i_d - E'_q\right)/T'_{d0}, \tag{14}$$

$$\dot{E}_{fd} = (K_A (V_{ref} - v + u_{pss}) - E_{fd})/T_A, \tag{15}$$

where:

$$P_e = v_d i_d + v_q i_q \quad v = \left(v_d^2 + v_q^2\right)^{1/2} \quad v_d = x_q i_q \quad v_q = E'_q - x'_d i_d$$

$$i_d = i_{Ed} + i_{Bd} + i_{TLd} \quad i_q = i_{Eq} + i_{Bq} + i_{TLq}.$$

Above, P_m is the mechanical input power of the generator; P_e is the electrical output power of the generator; M and D are the inertia constant and damping coefficient; ω_b is the synchronous speed of the generator; δ and ω are the rotor angle and speed; E'_q, E'_{fd}, and v are the generator internal voltage, field voltage, and terminal voltages, respectively; T'_{do} is the open-circuit field time constant; x_d, x'_d, and x_q are the generator reactance in the d-axis, d-axis transient reactance, and q-axis reactance, respectively; K_A and T_A are the gain and time constant of the generator exciter, respectively; V_{ref} is the AC bus reference voltage; and u_{pss} is the control signal of the PSS.

4. Linearized model of the power system

In this paper, in order to perform a stability evaluation, eigenvalue analysis is used. For this purpose and to obtain the eigenvalues of the system, the nonlinear dynamic equations of the test power system must be linearized around an operating point condition. Eqs. (16) through (20) show the linearized model of the test power system from Figure 2.

$$\Delta\dot{\delta} = \omega_b \Delta\omega \tag{16}$$

$$\Delta\dot{\omega} = \frac{1}{M}(\Delta P_m - \Delta P_e - D\Delta\omega) \tag{17}$$

$$\Delta\dot{E}'_q = \frac{1}{T'_{d0}}\left(-\Delta E'_q + \Delta E_{fd} + (x_d - x'_d)\Delta i_{1d}\right) \tag{18}$$

$$\Delta\dot{E}_{fd} = \frac{1}{T_A}(-\Delta E_{fd} + K_A(\Delta V_{tref} - \Delta V_t + \Delta u_{pss}) \tag{19}$$

$$\Delta\dot{V}_{dc} = K_7\Delta\delta + K_8\Delta E'_q - K_9\Delta V_{dc} + K_{ce}\Delta m + K_{c\delta e}\Delta\delta_E + K_{cb}\Delta m_B + K_{c\delta b}\Delta\delta_B \tag{20}$$

In the state-space representation, the power system can be modeled as:

$$\dot{x} = Ax + Bu, \tag{21}$$

where the state vector x, control vector u, state matrix A, and input matrix B are:

$$x = \begin{bmatrix} \Delta\delta & \Delta\omega & \Delta E'_q & \Delta E_{fd} & \Delta v_{dc} \end{bmatrix}^T,$$

$$u = \begin{bmatrix} \Delta u_{pss} & \Delta m_E & \Delta\delta_E & \Delta m_B & \Delta\delta_B \end{bmatrix}^T,$$

$$A = \begin{bmatrix} 0 & \omega_b & 0 & 0 & 0 \\ -\frac{k_1}{M} & -\frac{D}{M} & -\frac{k_2}{M} & 0 & -\frac{k_{pd}}{M} \\ -\frac{k_4}{T'_{do}} & 0 & -\frac{k_3}{T'_{do}} & \frac{1}{T'_{do}} & -\frac{k_{qd}}{T'_{do}} \\ -\frac{k_A k_5}{T_A} & 0 & -\frac{k_A k_6}{T_A} & -\frac{1}{T_A} & -\frac{k_A k_{vd}}{T_A} \\ k_7 & 0 & k_8 & 0 & -k_9 \end{bmatrix},$$

$$B = \begin{bmatrix} 0 & 0 & 0 & 0 & 0 \\ 0 & -\frac{k_{pe}}{M} & -\frac{k_{p\delta e}}{M} & -\frac{k_{pb}}{M} & -\frac{k_{p\delta b}}{M} \\ 0 & -\frac{k_{qe}}{T'_{do}} & -\frac{k_{q\delta e}}{T'_{do}} & -\frac{k_{qb}}{T'_{do}} & -\frac{k_{q\delta b}}{T'_{do}} \\ \frac{k_A}{T_A} & -\frac{k_A k_{ve}}{T_A} & -\frac{k_A k_{v\delta e}}{T_A} & -\frac{k_A k_{vb}}{T_A} & -\frac{k_A k_{v\delta b}}{T_A} \\ 0 & k_{ce} & k_{c\delta e} & k_{cb} & k_{c\delta b} \end{bmatrix}.$$

The linearized dynamic model of the state-space representation is shown in Figure 3.

4.1. UPFC-based damping controller

The damping controller is designed to produce an electrical torque, according to the phase compensation method, in phase with the speed deviation. In order to produce the damping torque, the 4 control parameters of the UPFC (m_E, δ_E, m_B, and δ_B) can be modulated.

In this paper, δ_E and m_B are modulated in order to damp the controller design. The speed deviation $\Delta\omega$ is chosen as the input to the damping controller. Figure 4 shows the structure of the UPFC-based damping controller. This controller may be considered as a lead-lag compensator. However, an electrical torque in phase with the speed deviation is to be produced to improve the damping of the power system oscillations. It consists of a gain block, signal-washout block, and lead-lag compensator. The parameters of the damping controller are obtained using the ICA technique.

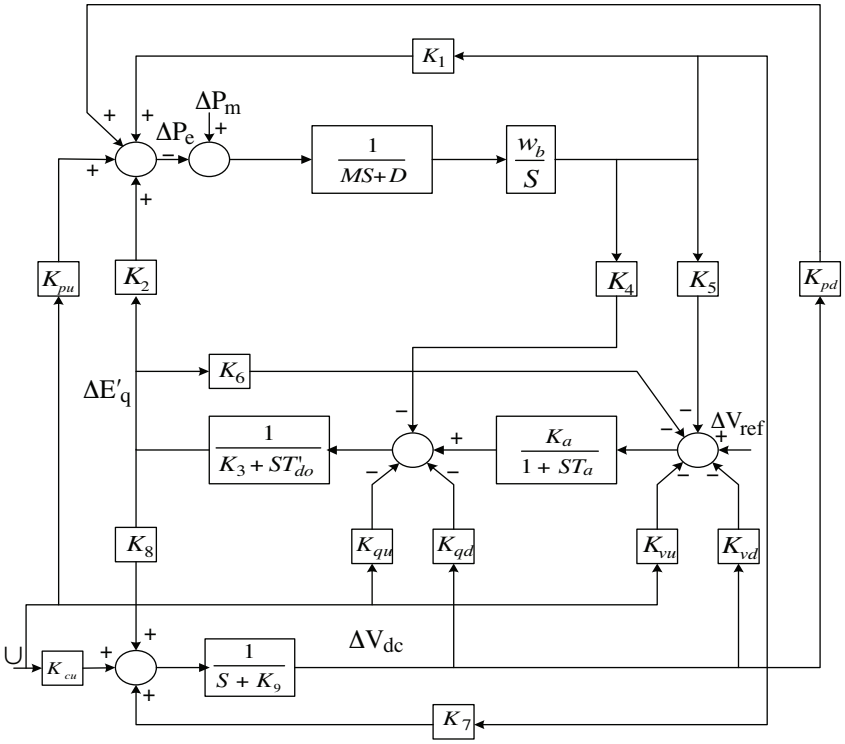

Figure 3. Modified Phillips-Heffron transfer function model [1].

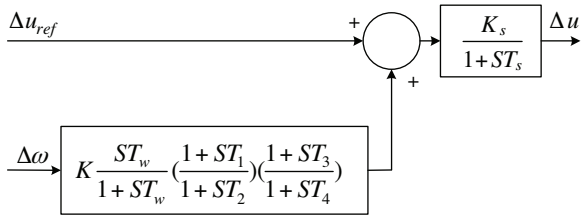

Figure 4. UPFC with a lead-lag controller.

4.2. UPFC controller design using the ICA

In the proposed method, the UPFC controller parameters must be tuned optimally to improve overall system dynamic stability in a robust way. This study employs the ICA to improve optimization synthesis and find the global optimum value of the fitness function in order to acquire an optimal combination. In this study, the ICA module works offline. In other words, the parameters of the UPFC damping controller are tuned for different loading conditions and system parameter uncertainties based on Table 1, and then the obtained optimal parameters of the damping controller are applied to the time-domain simulation.

For our optimization problem, an eigenvalue-based objective function reflecting the damping ratio is considered as follows:

$$J = \sum_{j=1}^{NP} (1 - \min(\xi_{ij})). \tag{22}$$

Table 1. System operating conditions and parameter uncertainties.

Loading conditions	P_e	Q_e	System parameter uncertainties
Nominal	1.000	0.015	No parameter uncertainties
Light	0.300	0.015	30% increase and decrease of line reactance X_T
Heavy	1.100	0.400	25% increase and decrease of machine inertia M
Leading power factor	0.700	–0.030	30% increase and decrease of field time constant T'_{do}

In Eq. (22), ξ_{ij} is the damping ratio of the ith eigenvalue of the jth operating point. NP is the total number of operating points for which the optimization is carried out. Given a complex eigenvalue $\sigma \pm \mu$, the damping ξ is defined as:

$$\xi = -\frac{\sigma}{\sqrt{\sigma^2 + \mu^2}}. \tag{23}$$

The parameters of UPFC-based controllers are optimized in order to have robust stabilizers over a wide range of operating conditions and system parameter uncertainties [16]. Four loading conditions, representing nominal, light, heavy, and leading power factor (PF), are taken into account. Each loading condition is considered with and without parameter uncertainties, as given in Table 1. Hence, the total number of points considered for the design process is 28, i.e. NP. The flowchart of the ICA technique is shown in Figure 5.

The optimization problem design can be formulated as the constrained problem shown below, where the constraints are the controller parameters bounds.

$$\text{Minimize } J$$

$$\text{Subject to}$$

$$\begin{aligned} K^{\min} &\le K \le K^{\max} \\ T_1^{\min} &\le T_1 \le T_1^{\max} \\ T_2^{\min} &\le T_2 \le T_2^{\max} \\ T_3^{\min} &\le T_3 \le T_3^{\max} \\ T_4^{\min} &\le T_4 \le T_4^{\max} \end{aligned} \tag{24}$$

Like the GA [24], in which every chromosome as a candidate solution includes a predefined number of genes, in the ICA, every country includes a predefined number of variables reflecting the country's characteristics, e.g., culture, language, and religion. In this study, the variables are a proportional gain and 4 time constants, as in Figure 6.

Typical ranges of the optimized parameters are [–100, 100] for K and [0.01, 1.5] for T_1, T_2, T_3, and T_4. The mentioned approach employs the ICA to solve this optimization problem and search for an optimal or near-optimal set of controller parameters.

5. Simulation results

5.1. Application of the ICA to the design process

The ICA was applied to search for the optimal parameter settings of the supplementary controllers in order to optimize the objective function. In order to acquire better performance, the number of countries, number of

initial imperialists, number of decades, assimilation coefficient (β), assimilation angle coefficient (γ), and ζ_{ica} were chosen as 30, 3, 300, 3, 0.3, and 0.2, respectively.

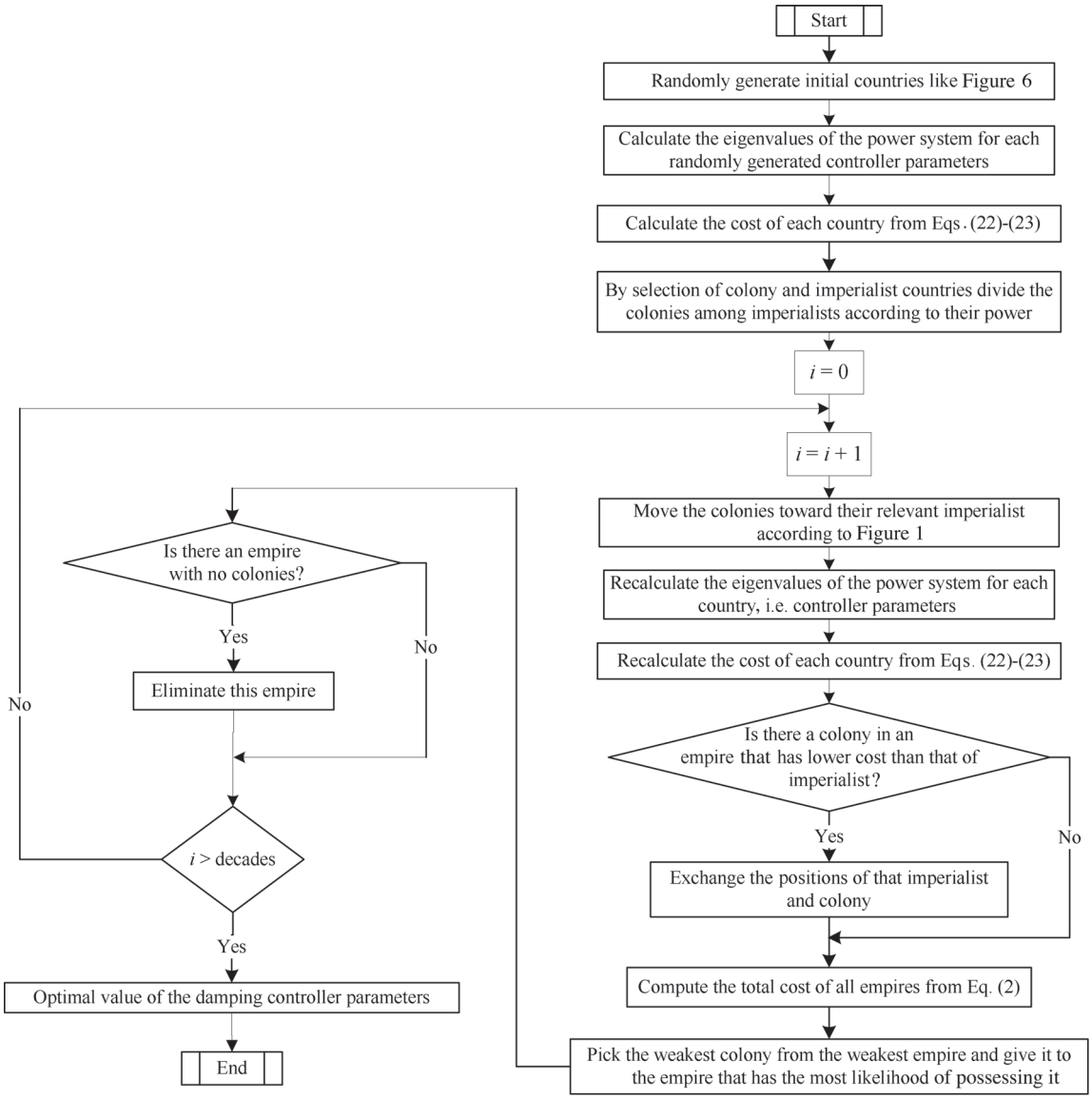

Figure 5. Flowchart of the implemented ICA technique in order to select optimal controller parameters.

k	T_1	T_2	T_3	T_4

Figure 6. Representation of a country in the optimization problem.

The final values of the optimized parameters with the objective function, for the 2 separate controllers, are given in Table 2. It should be noted that the optimization process was carried out for the system operating at different loading conditions and some parameter uncertainties, given in Table 1. The optimal parameters of the 2 controllers were found separately (Table 2). Figure 7 shows the illustration of cost versus iteration

for both the δ_E- and m_B-based controllers using the ICA technique. The minimum value for the δ_E-based controller is equal to 116.0625 and for the m_B-based controller is equal to 192.6712.

Table 2. Optimal parameters of the proposed controllers.

	K	T_1	T_2	T_3	T_4
m_B controller	100.0000	0.0500	0.5417	1.5000	0.0575
δ_E controller	–32.9829	0.0500	0.0540	0.0541	0.1368

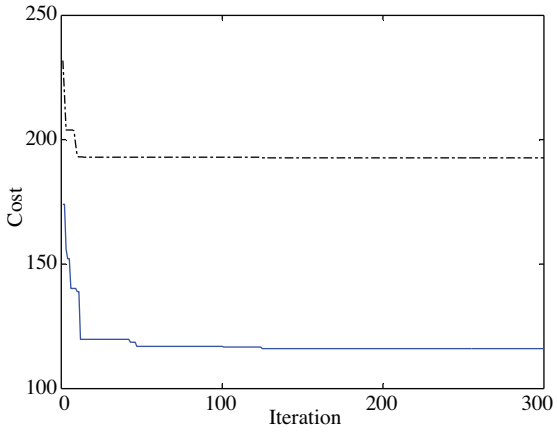

Figure 7. The convergence for objective function minimization using the ICA technique; solid line for δ_E-based controller and dash-dotted line for m_B-based controller.

5.2. Time-domain simulation

To assess the effectiveness of the proposed stabilizers, the system eigenvalues are obtained and a disturbance increase of 10% in the mechanical input power is considered in order to obtain the dynamic responses.

The system eigenvalues with and without the controllers at 4 different loading conditions are given in Table 3. It is clear that the open-loop system is unstable due to the fact that its electromechanical modes are in the right side of the s-plane. However, the proposed controllers dramatically stabilize the system. The electromechanical mode eigenvalues were shifted to the left in the s-plane and the system damping was greatly improved and enhanced with the proposed method.

System behavior due to the utilization of the proposed controllers was tested by applying a 10% step increase in mechanical input power at t = 0.1 s and a different loading condition. The system response to this disturbance under 4 different loading conditions for speed deviation, electrical power deviation, and internal voltage variations with δ_E- and m_B-based controllers, as well as without controllers, are shown in Figures 8-11. It can be seen that the proposed objective function-based optimized UPFC controller has good performance in damping low-frequency oscillations and stabilizes the system quickly. Furthermore, from the above conducted test, it can be concluded that the δ_E-based damping controller is superior to the m_B-based damping controller, which confirms the results of the singular value decomposition analysis carried out for the UPFC input signals in [1]. As the authors in that paper concluded, the best input signal of the UPFC damping controller is the excitation phase angle, i.e. δ_E.

Table 3. System eigenvalues and damping ratios with and without controllers at the 4 loading conditions.

	Nominal loading	Light loading	Heavy loading	Leading PF
Without controller	–15.7670 0.7848 ± *j*4.0065, –0.1922 –5.1875 –1.1339	–15.0467 0.1528 ± *j*3.7420, –0.0408 –5.2749 –0.4855	–15.5630 0.6940 ± *j*4.1985, –0.1631 –5.6580 –0.6817	–15.4593 0.5087 ± *j*3.8321, –0.1316 –5.0011 –1.0714
m_B-based controller	–17.5191 ± *j*2.0900, 0.9930 –1.5979 ± *j*5.2491, 0.2912 –1.4247 ± *j*1.5370, 0.6798 –1.0821 –0.2040	–15.9067 ± *j*0.1055, 1 –1.3268 ± *j*2.3718, 0.4882 –5.2876 –3.2462 –0.4854 –0.2040	–16.5795 ± *j*1.6945, 0.9948 –1.3693 ± *j*3.3577, 0.3776 –5.2717 –2.3711 –0.2051 –0.6826	–17.0526 ± *j*1.8776, 0.9940 –2.3584 ± *j*4.4488, 0.4684 –1.3805 ± *j*1.6676, 0.6377 –1.0215 –0.2037
δ_E-based controller	–18.5133 –15.7633 –2.6518 ± *j*3.7863, 0.5737 –1.8131 ± *j*1.9199, 0.6866 –4.9530 –0.1943	–18.5133 –15.0434 –2.6472 ± *j*4.3269, 0.5219 –5.9596 –2.2494 –0.8088 –0.1883	–15.5548 –18.5133 –4.2355 ± *j*0.7523, 0.9846 –2.3026 ± *j*4.4438, 0.4601 –1.1436 –0.1928	–15.4590 –18.5133 –2.8618 ± *j*4.1360, 0.5690 –1.3600 ± *j*1.5572, 0.6578 –5.5878 –0.1938

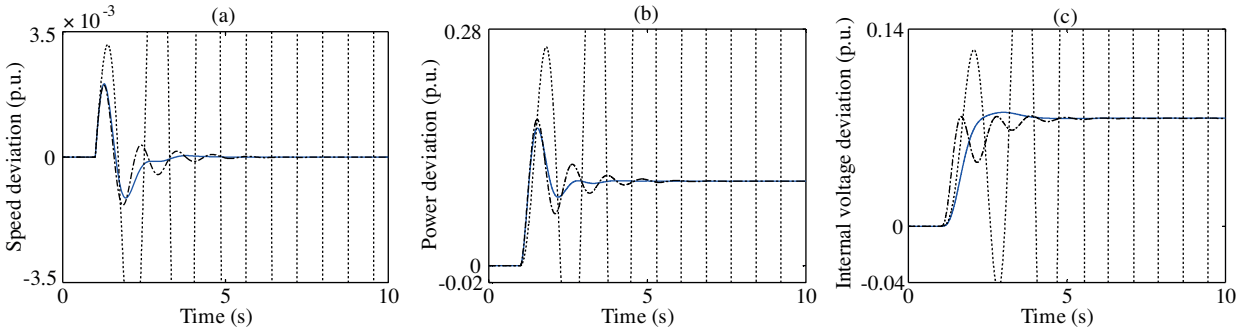

Figure 8. Dynamic responses to a 10% increase in mechanical input power for nominal loading conditions: (a) $\Delta\omega$, (b) ΔP_e, and (c) $\Delta E'_q$. Solid line: δ_E controller, dash-dotted line: m_B controller, dotted line: without controller.

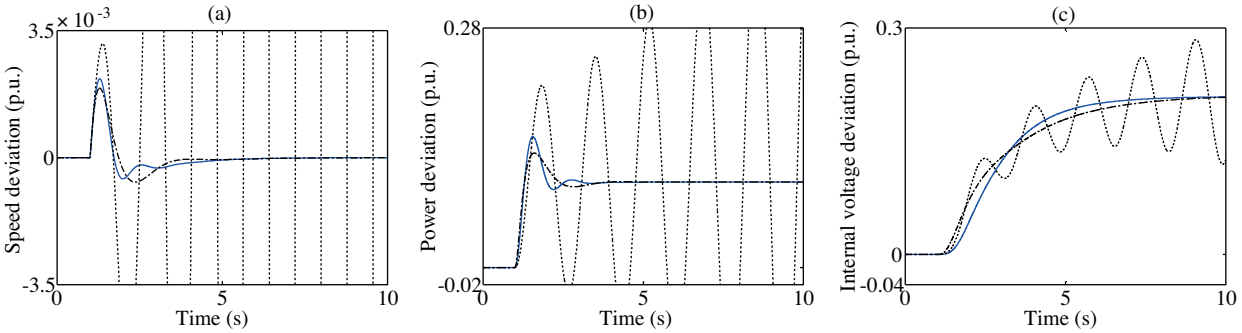

Figure 9. Dynamic responses to a 10% increase in mechanical input power for light loading conditions: (a) $\Delta\omega$, (b) ΔP_e, and (c) $\Delta E'_q$. Solid line: δ_E controller, dash-dotted line: m_B controller, dotted line: without controller.

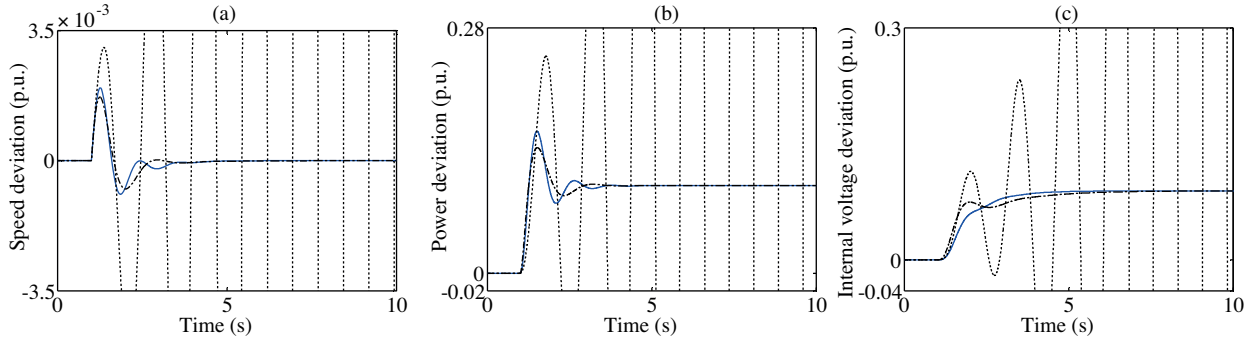

Figure 10. Dynamic responses to a 10% increase in mechanical input power for heavy loading conditions: (a) $\Delta\omega$, (b) ΔP_e, and (c) $\Delta E'_q$. Solid line: δ_E controller, dash-dotted line: m_B controller, dotted line: without controller.

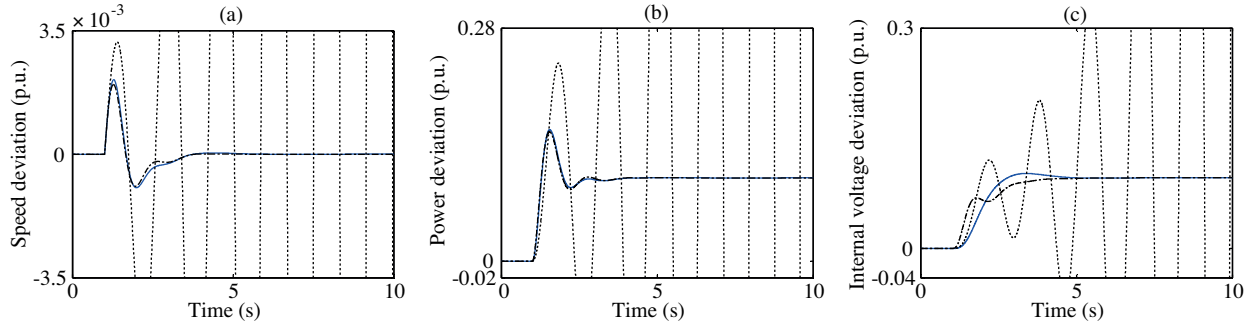

Figure 11. Dynamic responses to a 10% increase in mechanical input power for leading PF conditions: (a) $\Delta\omega$, (b) ΔP_e, and (c) $\Delta E'_q$. Solid line: δ_E controller, dash-dotted line: m_B controller, dotted line: without controller.

6. Conclusion

In this paper, low-frequency oscillation damping using a UPFC controller was investigated. The stabilizer was tuned to simultaneously shift the undamped electromechanical modes of the machine to the left side of the s-plane. An objective problem comprising the damping ratio of the undamped electromechanical modes was formulated to optimize the controller parameters. The design problem of the controller was converted into an optimization problem, which was solved using the ICA technique with the eigenvalue-based objective function.

The effectiveness of the proposed UPFC controller for damping low-frequency oscillations of a power system were demonstrated by a weakly connected example power system subjected to a disturbance: an increase in mechanical power. The eigenvalue analysis and time-domain simulation results showed the effectiveness of the proposed controller in damping low-frequency oscillations.

7. Appendix

The nominal parameters of the system are listed in Table 4.

Table 4. Test system parameters.

Generator	M = 8.0 MJ/MVA D = 0.0 T'_{do} = 5.044 s f = 60 Hz	v = 1.05 p.u. x_d = 1.0 p.u. x_q = 0.6 p.u. x'_d = 0.3 p.u.
Excitation system	K_A = 100	T_A = 0.01 s
Transformer	x_{tE} = 0.1 p.u.	
Transmission line	x_{BV} = 0.6 p.u.	x_T = 0.6 p.u.
UPFC	x_E = 0.1 p.u. x_B = 0.1 p.u. K_s = 1.0 T_s = 0.05 s	T_w = 5.0 s V_{dc} = 2 p.u. C_{dc} = 1 p.u.

References

[1] A.T. Al-Awami, Y.L. Abdel Magid, M.A. Abido, "A particle-swarm-based approach of power system stability enhancement with unified power flow controller", Electrical Power and Energy System, Vol. 29, pp. 251-259, 2007.

[2] L. Gyugyi, C.D. Schauder, S.L. Williams, T.R. Rietman, D.R. Torgerson, A. Edris, "The unified power flow controller: a new approach to power transmission control", IEEE Transactions on Power Delivery, Vol. 10, pp. 1085-1097, 1995.

[3] L. Gyugyi, "A unified power flow control concept for flexible AC transmission systems", IEE Proceedings - Generation Transmission Distribution, Vol. 139, pp. 323-333, 1992.

[4] A. Nabavi-Niaki, M.R. Iravani, "Steady-state and dynamic models of unified power flow controller (UPFC) for power system studies", IEEE Transactions on Power Systems, Vol. 11, pp. 1937-1943, 1996.

[5] P.C. Stefanov, A.M. Stankovic, "Modeling of UPFC operation under unbalanced conditions with dynamic phasors", IEEE Transactions on Power Systems, Vol. 17, pp. 395-403, 2002.

[6] H.F. Wang, "Damping function of unified power flow controller", IEE Proceedings - Generation Transmission Distribution, Vol. 146, pp. 81-87, 1999.

[7] H.F. Wang, "Application of modeling UPFC into multi-machine power systems", IEE Proceedings - Generation Transmission Distribution, Vol. 146, pp. 306-312, 1999.

[8] K.R. Padiyar, A.M. Kulkarni, "Control design and simulation of unified power flow controller", IEEE Transactions on Power Delivery, Vol. 13, pp. 1348-1354, 1997.

[9] E. Uzunovic, C.A. Canizares, J. Reeve, "EMTP studies of UPFC power oscillation damping", Proceedings of the North American Power Symposium, pp. 405-410, 1999.

[10] N. Mithulananthan, C. Canizares, J. Reeve, G. Rogers, "Comparison of PSS, SVC, and STATCOM for damping power system oscillations", IEEE Transaction on Power Systems, Vol. 18, pp. 786-792, 2003.

[11] R.K. Pandey, N.K. Singh, "Minimum singular value based identification of UPFC control parameters", IEEE Region 10 Conference, pp. 1-4, 2006.

[12] H. Shayeghi, H.A. Shayanfar, S. Jalilzadeh, A. Safari, "A PSO based unified power flow controller for damping of power system oscillations", Energy Conversion and Management, Vol. 50, pp. 2583-2592, 2009.

[13] A.K. Baliarsingh, S. Panda, A.K. Mohanty, C. Ardil, "UPFC supplementary controller design using real-coded genetic algorithm for damping low frequency oscillations in power systems", International Journal of Electrical Power and Energy Systems Engineering, Vol. 3, pp. 165-175, 2010.

[14] M. Tripathy, S. Mishra, G.K. Venayagamoorthy, "Bacteria foraging: a new tool for simultaneous robust design of UPFC controllers", International Joint Conference on Neural Networks, pp. 2274-2280, 2006.

[15] Y. Lee, S. Yung, "STATCOM controller design for power system stabilization with sub-optimal control strip pole assignment", International Journal of Electrical Power and Energy Systems, Vol. 24, pp. 771-779, 2002.

[16] H. Asadzadeh, "Damping of power system oscillations using UPFC based AIPSO-SA algorithm", MSc Thesis, Electrical Engineering Department of Azarbaijan University of Tarbiat Moallem, Iran, 2009.

[17] E. Atashpaz-Gargari, C. Lucas, "Imperialist competitive algorithm: an algorithm for optimization inspired by imperialistic competition", IEEE Congress on Evolutionary Computation, pp. 4661-4667, 2007.

[18] E. Atashpaz, F. Hashemzadeh, R. Rajabioun, C. Lucas, "Colonial competitive algorithm: a novel approach for PID controller design in MIMO distillation column process", International Journal of Intelligent Computing and Cybernetics, Vol. 1, pp. 337-355, 2008.

[19] R. Jahani, "Optimal placement of unified power flow controller in power system using imperialist competitive algorithm", Middle-East Journal of Scientific Research, Vol. 8, pp. 999-1007, 2011.

[20] H. Chahkandi Nejad, R. Jahani, "A new approach to economic load dispatch of power system using imperialist competitive algorithm", Australian Journal of Basic and Applied Sciences, Vol. 5, pp. 835-843, 2011.

[21] E. Bijami, J. Askari Marnani, S. Hosseinnia, "Power system stabilization using model predictive control based on imperialist competitive algorithm", International Journal on Technical and Physical Problems of Engineering, Vol. 3, pp. 45-51, 2011.

[22] M.H. Etesami, N. Farokhnia, S.H. Fathi, "A method based on imperialist competitive algorithm (ICA), aiming to mitigate harmonics in multilevel inverters", 2nd Power Electronics, Drive Systems and Technologies Conference, pp. 32-37, 2011.

[23] M.A. Abido, A.T. Al-Awami, Y.L. Abdel-Magid, "Power system stability enhancement using simultaneous design of damping controllers and internal controllers of a unified power flow controller", IEEE PES General Meeting, 2006.

[24] M. Mitchell, An Introduction to Genetic Algorithms, Cambridge, Massachusetts, MIT Press, 1999.